minerals

MDPI

Article

Instability Mechanism, Pressure Relief, and Long Anchorage Control Countermeasures for Surrounding Rock of Strong Mining Roadway at Large Mining Height Working Face

Deyu Qian [1,*], Hexi Jiao [1], Jinping Deng [1], Jingxuan Yang [1], Mingzhi Jiao [2], Guihong Xian [1], Chenshi Yu [1], Yingli Zhu [1], Jiale Liu [1], Sen Huang [1] and Binyong Li [1]

[1] School of Mines, China University of Mining and Technology, Xuzhou 221116, China
[2] The National Joint Engineering Laboratory of Internet Applied Technology of Mines, China University of Mining and Technology, Xuzhou 221116, China
* Correspondence: qian@cumt.edu.cn

Abstract: Double-roadway tunneling could mitigate the contradiction between mining production needs and tunneling speed, which is pivotal to the sustainable development of underground mines. However, it is very difficult to control the stability of a mining roadway on an adjacent working face suffering from strong mining disturbance due to double-roadway tunneling, especially at a large mining height working face. In order to control the stability of the return air roadway (RAR) 23205 of a strong mining roadway at working face 23205 in the Zhuanlongwan Coal Mine in Inner Mongolia, we carried out field monitoring, theoretical analysis, numerical simulations, and engineering practice to identify the main factors influencing the deformations and the stress distribution law of the surrounding rock in order to propose countermeasures for strong mining roadways. The results show the factors influencing the large deformation of strong mining roadways include large mining height, repeated mining, stress concentration due to the large coal pillar, and a small thickness of the anchorage layer in the roof. The stress peak in the central coal pillar caused by the first and second mining is 23.19 MPa and 27.49 MPa, respectively, and the stress concentration coefficients are 4.538 and 5.379, respectively. Countermeasures (pressure relief via large-diameter boreholes in the large coal pillar and long anchorage for roof reinforcement) were created to control the stability of a strong mining roadway, i.e., RAR 23205. Field measurements indicated that deformations in RAR 23205 could be efficiently controlled. The maximum deformation of the surrounding rock was 50 mm, which meets the safety and efficient production requirements of the coal mine. In addition, new roadway layout optimization and control countermeasures are put forward to control the stability of mining roadways.

Keywords: strong mining roadway; deformation and failure; stress evolution; pressure relief; bolt anchorage; large mining height

Citation: Qian, D.; Jiao, H.; Deng, J.; Yang, J.; Jiao, M.; Xian, G.; Yu, C.; Zhu, Y.; Liu, J.; Huang, S.; et al. Instability Mechanism, Pressure Relief, and Long Anchorage Control Countermeasures for Surrounding Rock of Strong Mining Roadway at Large Mining Height Working Face. *Minerals* **2023**, *13*, 391. https://doi.org/10.3390/min13030391

Academic Editor: Bekir Genc

Received: 27 February 2023
Revised: 8 March 2023
Accepted: 9 March 2023
Published: 10 March 2023

1. Introduction

There are many large important coalfields being developed in China, such as the Yushen, Shenfu, Ordos, and Datong mining areas, where the coal seams are thick and shallowly buried with relatively simple geological conditions, and the large underground coal mines with high output are characterized by fast mining speed and high mining intensity. In order to solve the contradiction between mining production needs and tunneling speed, the tunneling of double roadways with a large internal coal pillar of 15–30 m width is usually adopted. However, double-roadway tunneling causes the mining roadway at the adjacent working face to suffer from strong secondary mining disturbance. Under strong mining disturbance, many mining roadways have large deformations and experience failure of the surrounding rock, which leads to the instability of roadways and difficulty with maintenance [1–5]. In particular, the deformation and failure mechanisms and control of

strong mining roadways in a thick coal seam are more difficult. Large deformations and the failure of the surrounding rock in a strong mining roadway seriously restrict the production and efficiency of underground coal mines. Therefore, it is of practical significance to reveal the instability mechanism of the rock surrounding strong mining roadways and put forward countermeasures for ensuring the safety of mine production and reducing the huge economic cost of roadway repairs [6–8].

Many researchers have studied the deformation mechanisms and control technology of roadway-surrounding rock under different mining conditions. Krzysztof et al. [9] pointed out that the selection of roadway support should satisfy geometric, ventilation, and geomechanical criteria during the period of roadway excavation and mining. Kaiser et al. [10] measured the stress changes in the mining process of stope 5656 in Winston Lake Mine using multiple stress units and simulated the stress distribution of the roadway using the numerical calculation program MAP3D, and concluded that the reason for the roadway wall moving in and floor heave is the inelastic strain of the rock and the stress of the roadway transferred from the side to the bottom during excavation. Coggan et al. [11] put forward that the mudstone thickness of a weak roof under high horizontal stress had a significant impact on the overall failure degree of the roadway, which needed to be supported emphatically. Rezaei et al. [12] concluded that the nature of the surrounding rock of the roadway has a direct influence on the stress concentration coefficient. Wang et al. [13] selected 14 typical roadways (7 under dynamic pressure and 7 under static pressure) to investigate the characteristics of their excavation-damaged zone (EDZ). The results indicated that the EDZ width around roadways under dynamic pressure was larger than that under static pressure due to mining-induced disturbance and the effect of unstable overlying rocks in adjacent goafs. Osouli et al. [14] take the roof instability of underground coal mines in Illinois as an example, focusing on the interaction between roof rock unit bedding, the interaction between roof bolts and rock units, and the influence of water increase on roof deformation and failure. The results show that the roof failure is caused by the direct roof delamination caused by the large horizontal stress of the direct roof and the separation of the roof bolt from the rock mass. Gao et al. [15] proposed that the initial fracture of rock mass leads to the obvious expansion of cracks due to high mining stress. Luo et al. [16] illustrated how a reasonable blasting pressure relief scheme could improve the stress environment of rock surrounding roadways and reduce the risk of rock burst. Shen et al. [17] found that the displacement accelerated and the horizontal stress decreased significantly before roof collapse. Mo et al. [18] studied the floor heave management of Bulga's underground operation and the factors leading to floor behavior. The practical experience in mine shows that the floor failure is mainly caused by high horizontal stress, a large buried depth, and a weak floor lithologic structure. Frith et al. [19] proposed a prototype coal pillar and overburden system that used the in situ horizontal stress of the support system to reinforce the coal pillar through the surface protection member instead of simply hanging the anchor cable. Qin et al. [20] found that increasing the supporting strength of the internal bearing structure, cohesion, and internal friction angle of the surrounding rock and reducing the influence of mining can improve the bearing capacity of shallow surrounding rock. Yan et al. [21] characterized stress evolution during the process from roadway stability to instability under different lateral pressure conditions. On this basis, a single mechanically yieldable prop with high constant resistance was proposed to support the surrounding rock of retreating roadways in extra-thick coal seams. Xia et al. [22] investigated the dynamic mechanical state of the mining roadway with 6.0 m coal pillars under the influence of repeated mining. The results indicated that the coal pillar entered the residual state and that the solid coal side of the footwall panel became the main bearing coal mass under the abutment load caused by the mining. Kajzar et al. [23] used three-dimensional laser technology to monitor the ground displacement in underground excavation and monitored all the roof and side deformations during excavation. Sakhno et al. [24] obtained that the nonlinear deformation of the floor would cause obvious floor heave, demonstrated the peak plastic strain of the floor after bolt reinforcement by numeri-

cal simulation, and concluded that the depth of bolt reinforcement could be determined by the allowable floor heave. Fang and Li et al. [25,26] discussed the instability conditions of a lower coal roadway affected by multiple mining disturbances during the mining of a close-distance coal seam group and put forward effective countermeasures to ensure stability control. Vardar et al. [27] found that the impact tendency of mining depth on roadway excavation can reach more than twice that of the non-fault model, and geological faults in different positions may interact with roadway excavation.

The above results provide important contributions to mining roadway support research. However, stability control of the rock surrounding strong mining roadways due to repeated mining in a large mining height working face is extremely difficult, which affects the safety of underground coal mines. Based on the engineering background of strong mining roadways, for a return air roadway 23205 (RAR 23205) suffering repeated mining in a thick coal seam in Zhuanlongwan Coal Mine in Inner Mongolia (Figure 1), numerical simulation, engineering practice, and field measurements were used to: analyze the factors influencing the large deformation and failure of rock surrounding a strong mining roadway; reveal the large deformation and instability mechanisms of the surrounding rock; and propose countermeasures for control stability. The originality of this study includes the evolution law of mining stress and displacement of surrounding rock during double-roadway tunneling and the first and second mining, and integrated stability control schemes of pressure relief and anchorage for strong mining roadways. This study is of practical significance for the stability control of roadways due to repeated mining in underground coal mines.

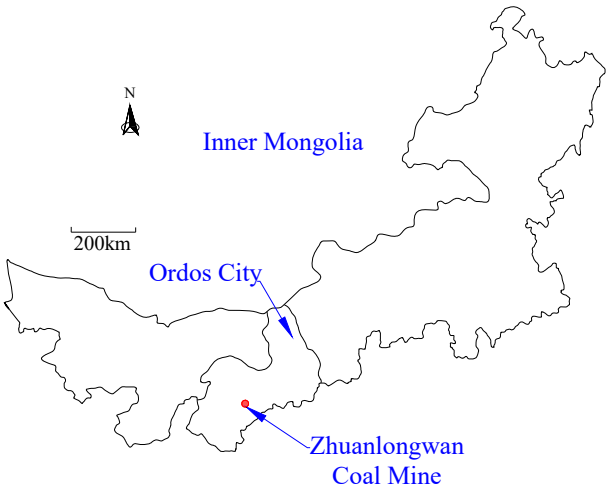

Figure 1. Location of Zhuanlongwan Coal Mine in Inner Mongolia.

2. Engineering Geological Profiles and Deformation Failure Characteristics of Strong Mining Roadways

2.1. Engineering Geology of Strong Mining Roadways

Working face 23204 is located in Mining Area No. 2 in Zhuanlongwan Coal Mine, Inner Mongolia (Figure 2). The thickness of coal seam II-3 is between 3.68 m and 5.25 m (average: 4.82 m). The coal seam is generally high in the east and low in the west, high in the north and low in the south. The dip angle of the coal seam is 0°–3°, and the average dip angle is 1°. The length of the working face along the strike direction is 5753.4 m. The inclination width is 294 m. RAR 23205, i.e., auxiliary transport roadway 23204 and haulage roadway 23204 (HR 23204), are synchronously tunneled, affected by the first mining of working face 23204 and the second mining of working face 23205. The borehole core column is shown in Figure 3.

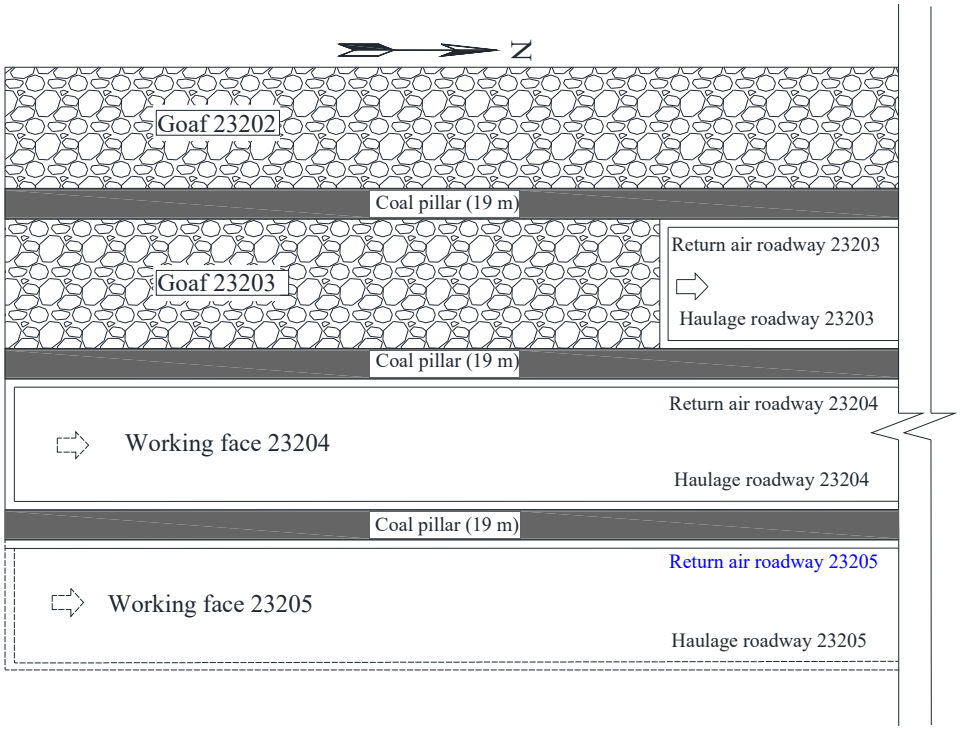

Figure 2. Location relationship of RAR 23205.

Thickness /m	Buried depth/m	Lithology	Description	Borehole column
12.51	94.97	Sandstone	White gray, layered structure, argillaceous cementation.	
3.03	98	Muddy siltstone	White gray, layered structure, mica content is higher.	
22.25	120.25	Sandstone	Gray - white, layered structure, bedding development.	
3.86	124.11	Mudstone	Gray-white, layered structure.	
5.84	129.95	Sandstone	Gray-white, gray-green, yellow-green, layered structure.	
1.79	131.74	Coal II-3(1)	Black, layered structure, broken.	
3.60	135.34	Fine sandstone	Gray-white, layered structure.	
10.44	145.78	Silty mudstone	Gray, massive structure, argillaceous cementation.	
4.80	150.58	Coal II-3	Black, layered structure, broken.	
2.26	152.84	Muddy siltstone	Gray, block structure.	
0.98	153.82	Coal II-4	Black, layered structure, broken.	
10.94	164.76	Sandstone	Gray-white, layered structure.	
1.90	166.66	Mudstone	Light gray, layered structure.	
1.74	168.40	Coal III-2	Black, layered structure, intact.	
4.33	172.73	Silty sandstone	Gray-white, layered structure.	

Figure 3. Borehole core column.

2.2. Original Support Scheme for Strong Mining Roadway RAR 23205 during Tunneling

RAR 23205 of a strong mining roadway was constructed by a tunneling and anchoring machine. The tunneling section was 5600 mm wide and 3950 mm high, and the net section after support was 5400 mm wide and 3600 mm high (Figure 3).

1. Roof Support

The original roadway support scheme is shown in Figure 4.

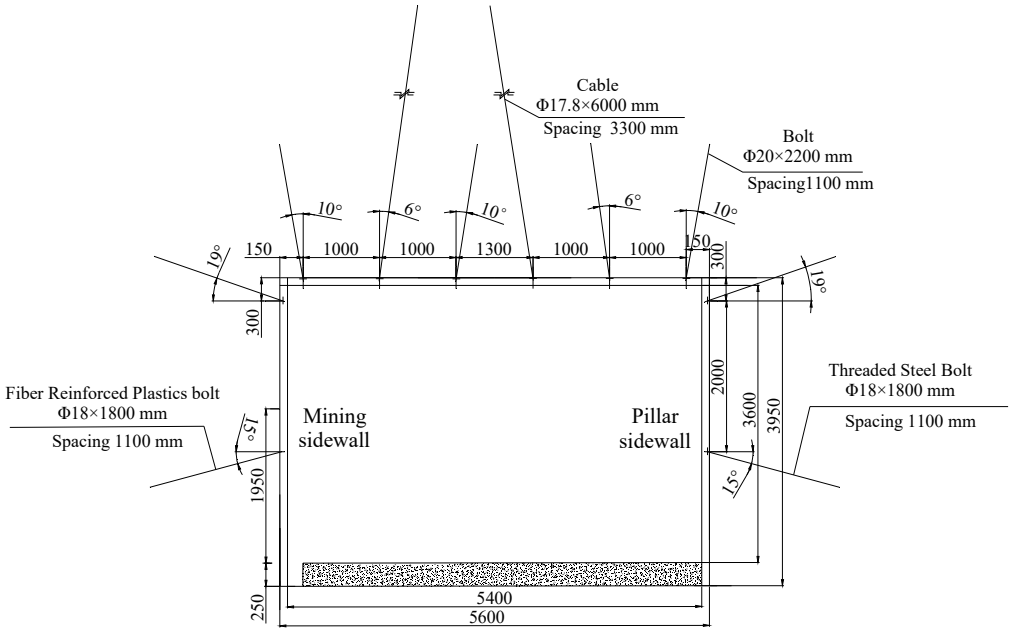

Figure 4. Original support scheme of RAR 23205.

The roof was supported by six bolts, each 20 mm in diameter and 2200 mm in length, combined with two cables, each 17.8 mm in diameter and 6000 mm in length. A resin anchorage agent of MSCKb2570 was used for anchoring each bolt. Two resin anchorage agents of MSCKb2570 were used for anchoring each cable. The spacing of bolts and cables was 1000 and 2300 mm, respectively. The interval spacing of bolts and cables along the roadway axis was 1100 and 3300 mm, respectively.

2. The Pillar Sidewall and The Mining Sidewall

The pillar sidewall was supported by two threaded steel bolts, each 18 mm in diameter and 1800 mm in length. The mining sidewall was supported by two fiberglass-reinforced plastic (FRP) bolts, each 18 mm in diameter and 1800 mm in length. A resin anchorage agent of MSCKb2570 was used for anchorage for each bolt. The interval spacing of all bolts in the sidewalls along the roadway axis was 1100 mm.

2.3. Deformation and Failure Characteristics of Strong Mining Roadways

According to the field investigation results of return air roadway 23204 (RAR 23204) in Zhuanlongwan Coal Mine, there was serious floor heave, floor cracking, bolt and cable failure, and integral displacement of the pillar sidewall. After the first mining, a large number of roof cables in RAR 23204 failed, there was severe subsidence of the roof, and both sides were severely damaged. Even with overall maintenance of the roadway, it was difficult to ensure safe production. The deformation and failure characteristics of the roadway are listed below.

1. Roof broken and stepped severe subsidence

As shown in Figure 5a, stepped roof subsidence and mining sidewall failure occurred. A bedding fracture of the coal body developed, which often causes delamination damage

and collapse. The tensile stress concentrated in the middle of the roof due to the large section span, as was the delamination damage range. The roof subsidence in the local area was up to 700 mm, and the roof separation was up to 80 mm.

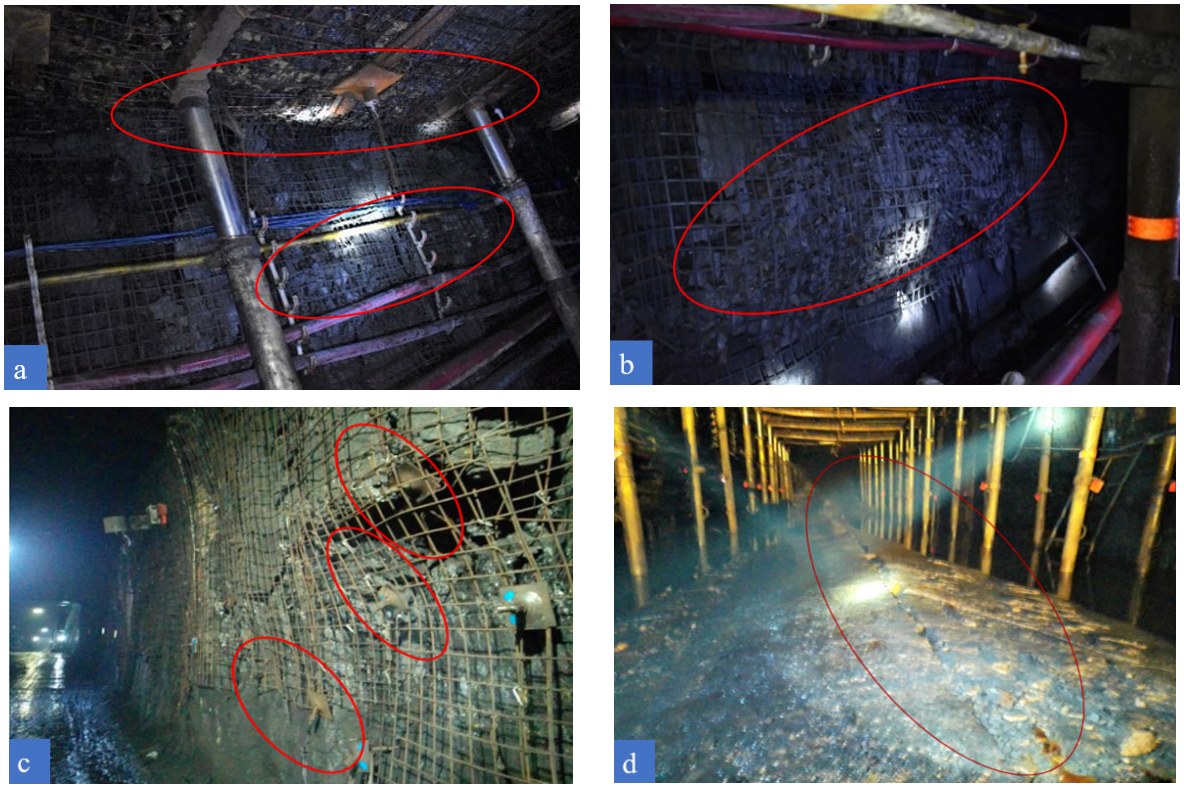

Figure 5. Failure characteristics of a strong mining roadway in RAR 23204: (**a**) stepped roof subsidence and mining sidewall failure; (**b**) failure instability of mining sidewall; (**c**) pillar sidewall failure instability and bolt failure; (**d**) severe floor heaving and floor cracking.

2. Failure and Instability of Two Sides of The Roadway

As shown in Figure 5a–c, the mining sidewall of RAR 23204 under the influence of severe mining showed a large area of failure and instability and the failure of a large number of bolts. Under the action of strong disturbance and mining stress, the stress concentration of the roadway shoulder angle was high. The local roof was completely cut at the shoulder angle, the coal–rock mass was broken and collapsed, and the roof was netted.

3. Severe Floor Heaving

As shown in Figure 5d, the coal roadway with a large mining height and large section was affected by strong mining: the abutment pressure of the coal rib increased sharply, and the stress was transmitted to the no-support floor through the coal rib. The mining stress caused floor cracking and severe floor heaving, which affect traffic and safety.

3. Factors Influencing Large Deformation and Failure of Surrounding Rock of Strong Mining Roadway

3.1. Large Mining Height

The average mining height of working faces is 4.8 m. The average daily mining progress is about 14 m. The large average mining height and the fact that the roof caved in naturally after coal mining cause the height of the basic roof fracture to increase. The rotary subsidence of the above block to the edge of the coal pillar causes the concentration of mining stress on the coal side, which aggravates the development of the surrounding rock fracture and transfers from shallow to deep to form a large deformation of the surrounding rock.

3.2. Repeated Mining

The working face in the second mining area of Zhuanlongwan Coal Mine was successively replaced, with three roadways arranged in one working face and two roadways tunneled at the same time. RAR 23204 was affected by the two mining operations working faces, 23203 and 23204. The deformation and failure of the surrounding rock were serious, and the maintenance was difficult.

3.3. Stress Concentration in the Large Coal Pillar

The width of the coal pillar is 19 m between roadways. When the working face is mined, the coal pillar is in the area of increasing abutment pressure. High concentrated stress causes the development of a plastic zone, the decrease of coal and rock strength, the crushing of coal and rock mass, and the failure of the support system. The stress concentration of a large coal pillar increases the difficulty of roadway maintenance.

3.4. Small Thickness of Anchorage Layer in the Roof

The borehole detection results of the roof-surrounding rock are shown in Figure 6. There were many transverse and longitudinal cracks in the roof of RAR 23204 within 5 m. The cracks in some sections were more than 6 m, and there were large separations and fracture zones in some sections. The length of the supporting bolt was 2.2 m, and 6 m cable was used in some sections. Due to the short length of the bolt and the large number of separations outside the anchorage zone, the thickness of the roadway roof anchorage circle was small, and the anchorage system had weak resistance to mining, so it could not achieve the maintenance effect of coordinated bearing.

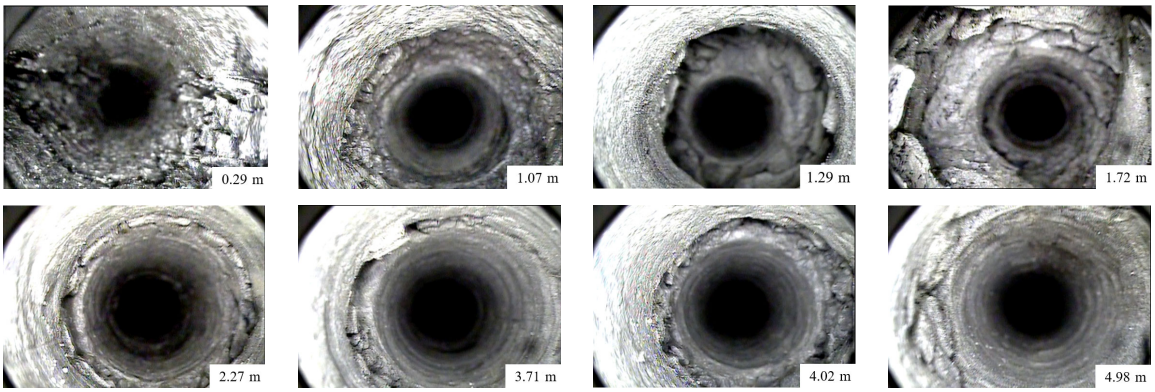

Figure 6. Borehole imaging of roof-surrounding rock of RAR 23204.

4. Large Deformation and Instability Mechanism of Surrounding Rock of Strong Mining Roadways

4.1. Model Establishment

According to the actual engineering geological conditions, the FLAC3D numerical model was established, as shown in Figure 7. The physical and mechanical parameters of coal and rock are shown in Table 1. The model's size was (length × width × height) 330 m × 100 m × 78 m. The vertical stress was 3.81 MPa at the top of the model, and the horizontal stress was 4.5 MPa according to field measurement. The bottom boundary of the model was fixed in the vertical direction, and the left and right boundaries were fixed in the horizontal direction. The model adopted the Mohr–Coulomb criterion.

4.2. Simulation Schemes

The mining sequence of the working face in the model is shown in Figure 8a, and the specific simulation contents were as follows:

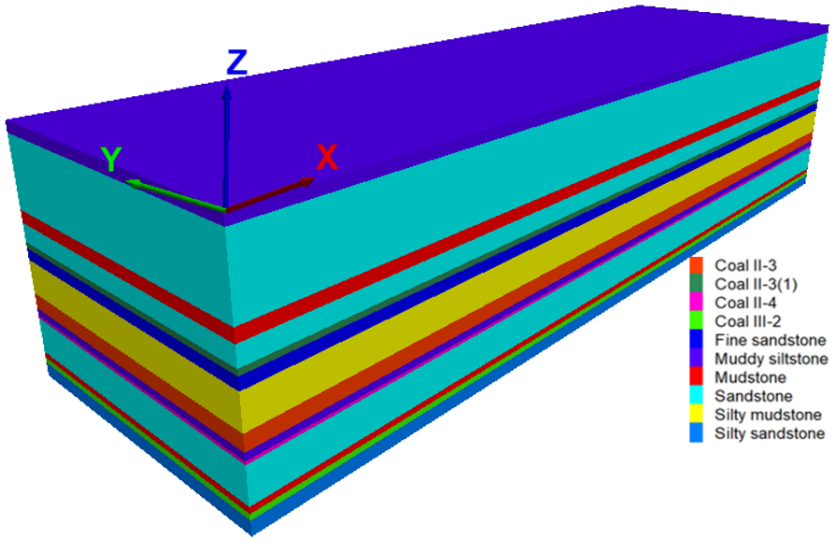

Figure 7. Numerical model.

Table 1. Physical and mechanical parameters of coal–rock mass.

Lithology	Thickness (m)	Density (kg·m^{-3})	Bulk Modulus (GPa)	Shear Modulus (GPa)	Angle of Internal Friction (°)	Cohesion (MPa)	Tensile Strength (MPa)
Sandstone	12.51	2670	6.05	1.35	38.33	5.44	3.89
Muddy siltstone	3.03	2387	4.86	2.43	35.1	2.9	2.18
Sandstone	22.25	2670	6.05	1.35	38.33	5.44	3.89
Mudstone	3.86	2325	5.05	2.66	34.76	3.4	2.05
Sandstone	5.84	2670	6.05	1.35	38.33	5.44	3.89
Coal II-3(1)	1.79	1430	1.32	0.49	30	2.5	1.8
Fine sandstone	3.60	2365	2.73	1.41	33.95	5.5	3.18
Silty mudstone	10.44	2387	2.01	1.98	35.1	2.9	3.41
Coal II-3	4.80	1430	1.32	0.49	30	2.5	1.8
Muddy siltstone	2.26	2387	4.86	2.43	35.1	2.9	2.18
Coal II-4	0.98	1430	1.32	0.49	30	2.5	1.8
Sandstone	10.94	2670	6.05	1.35	38.33	5.44	3.89
Mudstone	1.90	2325	5.05	2.66	34.76	3.4	2.05
Coal III-2	1.74	1430	1.32	0.49	30	2.5	1.8
Silty sandstone	4.33	2219	5.0	2.78	37.62	2.2	1.97

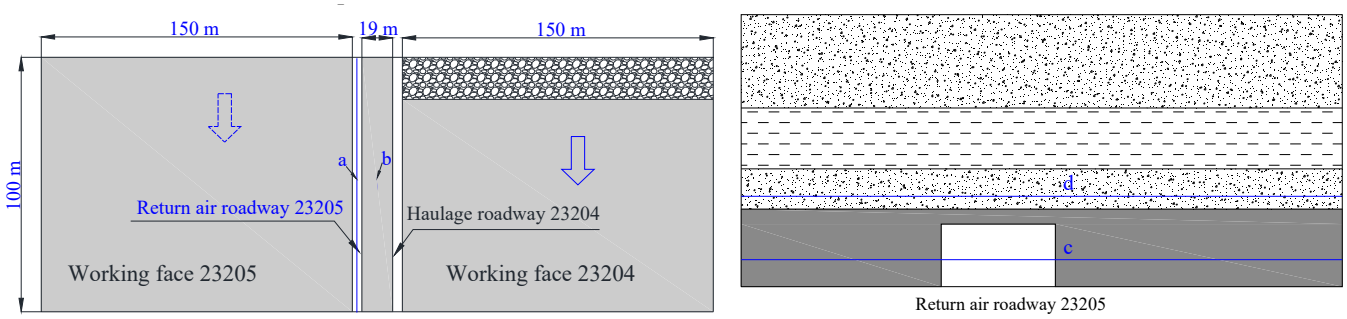

Figure 8. Mining sequence and monitoring lines layout of the working face: (**a**) strike monitoring lines' layout and simulation scheme; (**b**) inclination monitoring lines' layout.

1. The stress evolution and displacement distribution laws of the rock surrounding RAR 23205 without support during the tunneling were simulated and analyzed;
2. The stress evolution and displacement distribution of rock surrounding RAR 23205 without support under the first mining disturbance of working face 23204 were simulated;
3. The stress evolution and displacement distribution of rock surrounding RAR 23205 without support under the second mining disturbance of working face 23205 were simulated.

In order to quantitatively analyze the stress evolution law of the surrounding rock after coal seam mining, measuring lines were arranged along the strike and inclination directions, as shown in Figure 8. The measuring lines along the strike were arranged in front of the tunneling, namely measuring line a. Measuring line b was located 2 m along the roof, in the middle of the coal pillar. The measuring lines along the inclination were arranged in the middle of the roadway and 2 m along the roof, namely measuring lines c and d.

The stress distribution in the front of the tunneling of RAR 23205 was obtained by monitoring line a; the vertical stress distribution at 2 m of the roof of RAR 23205 in the front of the mining working face 23204 with different mining distances during the first mining was obtained by monitoring line b. Through monitoring line c, the vertical stress distribution in the middle of the RAR 23205 was obtained during the tunneling, the first mining period of working face 23204, and the second mining period of working face 23205. The vertical stress distribution of 2 m along the roof of RAR 23205 during the second mining was obtained with monitoring lines.

4.3. Stress Evolution Law of Surrounding Rock of Strong Mining Roadways

4.3.1. Stress Evolution during Tunneling

The stress distribution in the front of the tunneling working face of RAR 23205 is shown in Figure 9a; after the completion of the double tunneling, the stress distribution in the middle of RAR 23205 is shown in Figure 9b.

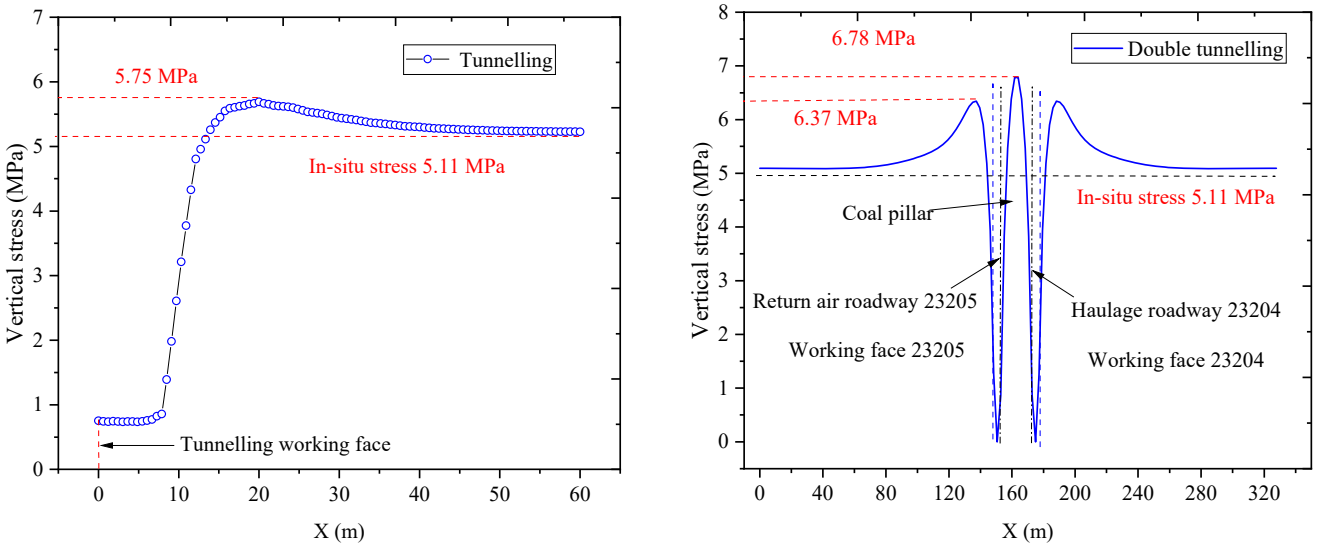

Figure 9. The stress evolution law of the surrounding rock during the tunneling: (**a**) stress distribution in the front of the tunneling; (**b**) stress distribution in the middle of the roadway after the tunneling.

It can be seen from Figure 9a that, due to the influence of the tunneling disturbance, the stress in the front of the tunnel was in a dynamic adjustment process. The coal body in the front of the tunnel was broken to form a plastic zone, and the range of the plastic zone was about 5 m. Subsequently, stress increased rapidly. The maximum stress was 15 m in the front of the tunneling working face, the peak stress was 5.75 MPa, and the stress concentration coefficient was 1.125. Subsequently, the stress decreased slowly, and the 40 m in the front of the tunneling working face was reduced to the in situ stress.

It can be seen from Figure 9b that the stress in the coal pillar and working faces 23204 and 23205 was symmetrically distributed after HR 23204 and RAR 23205 tunneling. The stress in the coal pillar was significantly higher than that in the working face. The peak stress in the coal pillar was 6.78 MPa, and the stress concentration coefficient was 1.327. The peak stress was in the middle of the coal pillar, 9.5 m away from the sidewall of the

roadway. The peak stress on the solid coal side at HR 23204 and RAR 23205 was 6.37 MPa, and the stress concentration coefficient was 1.247, 12 m away from the roadway side.

4.3.2. Stress Evolution during the First Mining

According to the field measurement of the initial weighting interval of 40 m during the mining period of working face 23204, the stress distribution law of the surrounding rock was simulated for 25 m and 50 m along working face 23204.

During the first mining, the vertical stress distribution was 2 m along the roof of RAR 23205 in the front of the working face 23204 with different mining distances, as shown in Figure 10a, and the vertical stress distribution in the middle of RAR 23205 is shown in Figure 10b.

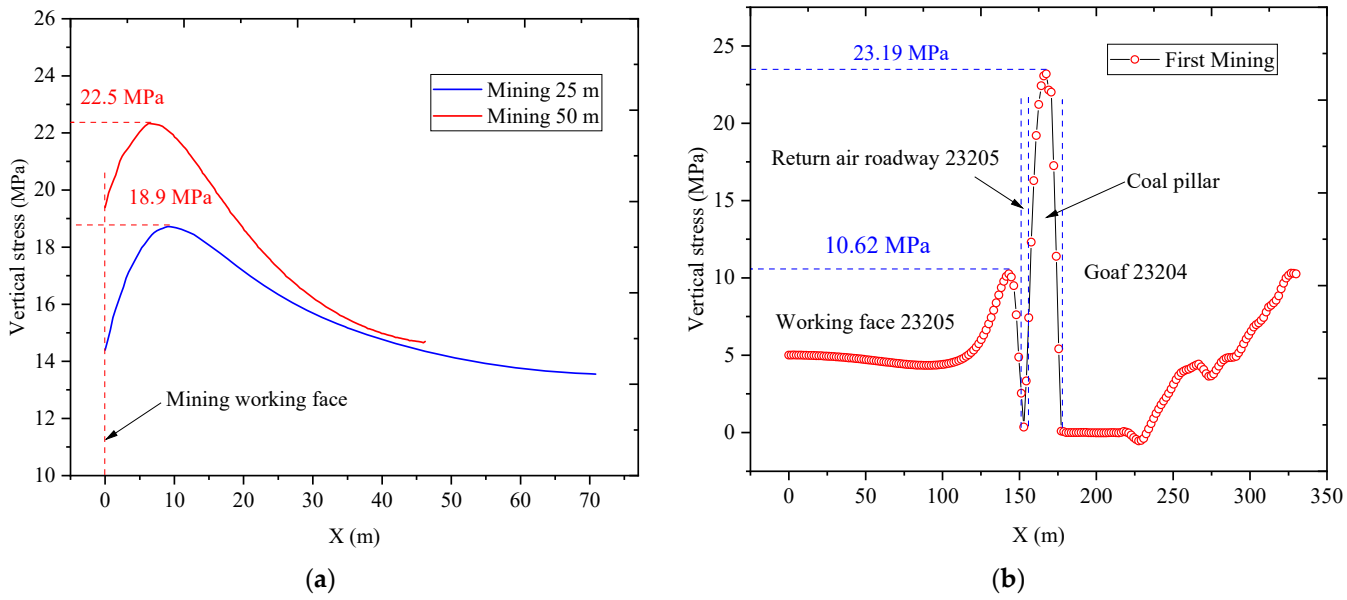

Figure 10. Stress evolution law of surrounding rock during the first mining: (**a**) the vertical stress distribution at 2 m from the roof in the middle of the coal pillar in the front of the working face with different mining distances; (**b**) the vertical stress distribution in the middle sidewalls of RAR 23205.

It can be seen from Figure 10a that the influence of mining not only formed a stress concentration in the coal pillar but also caused an increase in stress near the goaf in the front of the mining face. The stress concentration area moved forward with the mining of the working face. Due to the influence of mining disturbance, the coal mass in the mining face was loose and broke to form a plastic zone; the stress increased rapidly in the front of the working face, reached a peak at 8–9 m in the front of the working face, and then decreased gradually. The peak stress was 18.8 MPa and 22.3 MPa at 25 m and 50 m of the working face, respectively. The roof did not collapse at 25 m of the working face mining. Therefore, the stress disturbance was significantly less than that at 50 m of working face mining. Although the stress peak was different due to different engineering disturbance intensities, the stress evolution laws were the same.

According to Figure 10b, the movement space caused by roof breaking due to the mining effect was sufficient, and the stress in the coal pillar increased sharply due to the strong disturbance. The peak stress was 23.19 MPa, and the stress concentration coefficient reached 4.538. The peak stress was 6 m away from the pillar sidewall of goaf 23204 and 13 m away from the pillar sidewall of RAR 23205, and the peak position range was 9–13 m. The peak stress of the mining sidewall was 10.62 MPa, the stress concentration coefficient was 2.078, and the stress was only 45.8% of the pillar sidewall. The peak stress was 6.2 m from the roadway. The influence of the main roof fracture on the mining sidewall was significantly less than that of the pillar sidewall when working face 23204 was mined, but the peak stress of the roadway was significantly greater than that of the tunneling period.

4.3.3. Stress Evolution during the Second Mining

During the second mining of working face 23205, the vertical stress distribution in the middle of the roadway and 2 m along the roof of RAR 23205 is shown in Figure 11a,b respectively.

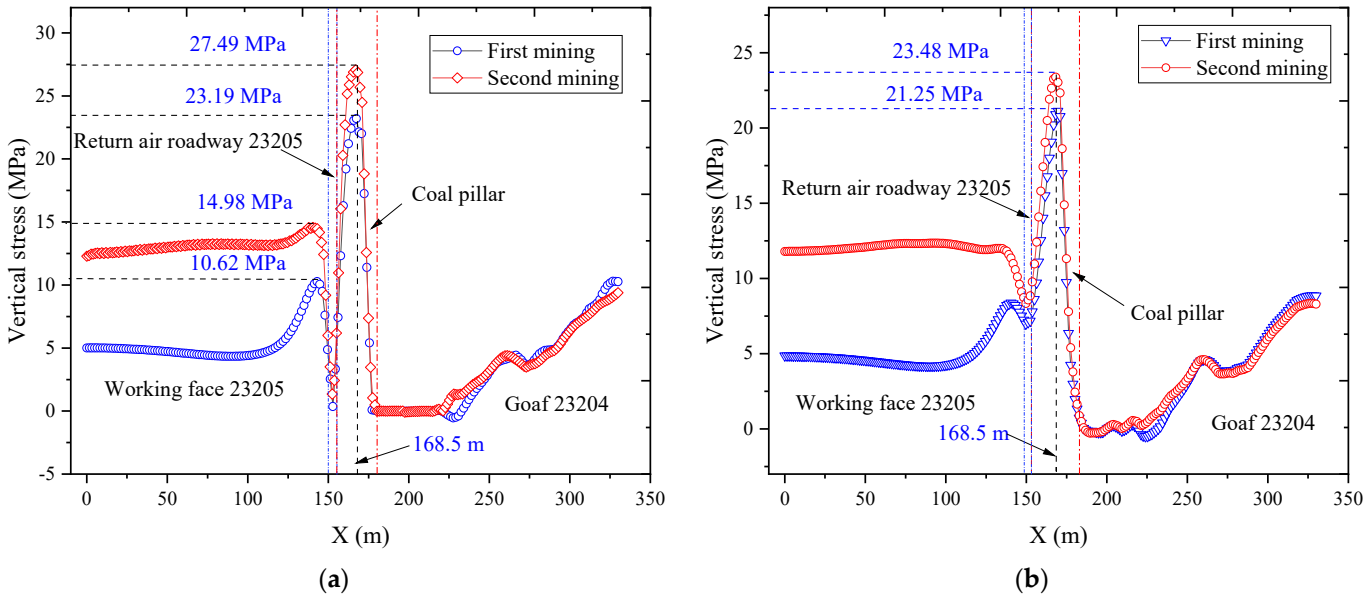

Figure 11. Stress evolution law of surrounding rock during the second mining of working face 23205: (**a**) the vertical stress distribution in the middle sidewalls of RAR 23205; (**b**) the vertical stress distribution 2 m along the roof of RAR 23205.

When RAR 23205 was disturbed by mining, the peak stress in the middle of the roadway was significantly higher than that on the roof. It can be seen from Figure 11a that, after the mining of the working face 23204, with the initial breaking and the periodic weighting of the roof, the cantilever beam structure of the goaf caused the stress to increase sharply in the front of the working face. The peak stress of the coal pillar under the first mining was 23.19 MPa, and the stress concentration coefficient was 4.538. In the mining process of working face 23205, the peak stress in the coal pillar increased again; the peak value reached 27.49 MPa, and the stress concentration coefficient increased to 5.379. Compared with the first mining period, the stress increased by 18.54% during the second mining period; the peak stress in the coal pillar was 10.5 m away from the pillar sidewall and 8.5 m away from the goaf. The peak stress range of the coal pillar during the first mining and the second mining was 8–13 m and 7–13 m, respectively. The stress peak values of the solid coal side during the first mining and the second stress were 10.62 MPa and 14.98 MPa, respectively. Compared with the first mining period, the peak stress during the second mining period increased by 41.05%. The peak stress point moved from 9 m to 11 m away from RAR 23205, i.e., it moved 2 m deeper into the coal body.

It can be seen from Figure 11b that, after the mining of working face 23204, the peak stress in the coal pillar at 2 m of the roof was 21.25 MPa, and the stress concentration coefficient was 4.159. During the mining process of working face 23205, the peak stress in the coal pillar increased to 23.48 MPa, and the stress concentration coefficient was 4.595. Compared with the first mining, the stress increased by 10.49% during the second mining.

Comprehensive analysis shows that the influence of the second mining disturbance on RAR 23205 was more severe. The damage caused by the lateral abutment pressure caused by the second mining on the roadway-surrounding rock was far greater than that caused by the tunneling and first mining. There was a trend of sudden instability for roadway-surrounding rock, and the difficulty of road maintenance significantly increased.

4.4. Displacement Distribution Law of Roadway-Surrounding Rock under Strong Mining

4.4.1. Displacement Distribution of Surrounding Rock after Tunneling

The displacement distribution of the roadway after double tunneling is shown in Figure 12.

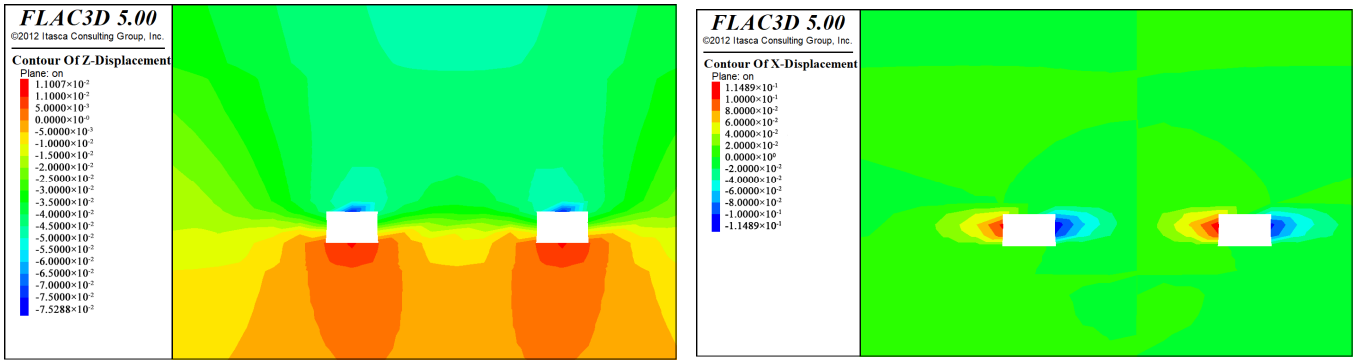

(**a**) (**b**)

Figure 12. Displacement distribution of roadways after tunneling: (**a**) vertical displacement distribution; (**b**) horizontal displacement distribution.

It can be seen in Figure 12 that the roof subsidence of RAR 23205 was 75.29 mm, the floor heave was 11.01 mm, and the deformation of the mining sidewall and pillar sidewall was 104.89 mm after the double tunneling. The deformation of the roadway-surrounding rock was mainly in the horizontal direction during the tunneling; the deformation trend of the surrounding rock of HR 23204 was the same as that of RAR 23205, and the deformation was symmetrical with respect to the coal pillar.

4.4.2. Displacement Distribution of Surrounding Rock after the First Mining

The distribution law of surrounding rock displacement of RAR 23205 after the mining of working face 232004 is shown in Figure 13.

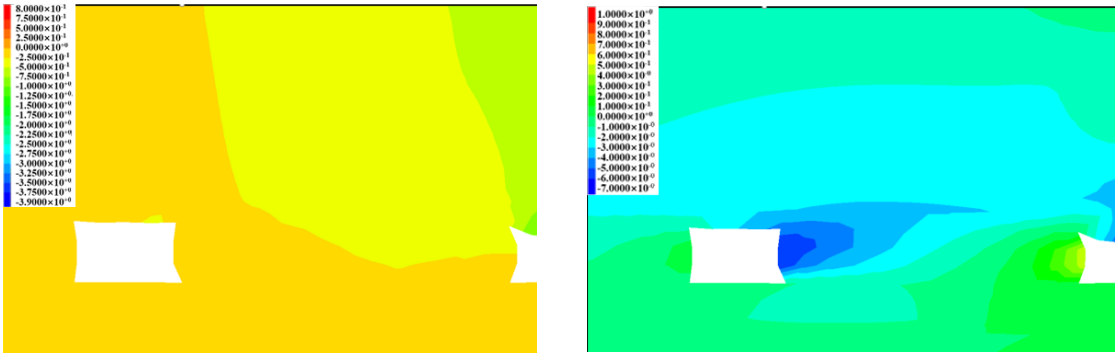

(**a**) (**b**)

Figure 13. Displacement distribution of RAR 23205 after first mining: (**a**) vertical displacement distribution; (**b**) horizontal displacement distribution.

In Figure 13, it can be seen that the disturbance of working face 23204 mining on the roadway was much greater than that of the tunneling. After first mining, the deformation of the rock surrounding RAR 23205 increased greatly: the roof deformation reached 262.9 mm, and the floor heave was 64.9 mm. The cumulative deformation of the mining sidewall and the pillar sidewall reached 133.5 mm and 563.4 mm, respectively. Compared with the tunneling period, the subsidence of roadway roofs and the deformation of pillar sidewalls significantly increased, so the support of the roof and pillar sidewall should be strengthened or reinforced before the first mining.

4.4.3. Displacement Distribution of Surrounding Rock after the Second Mining

The surrounding rock deformation statistics of the double tunneling, working face mining 23204 (the first mining) and working face mining 23205 (the second mining) are summarized in Table 2.

Table 2. Deformation of the roadway-surrounding rock under different engineering disturbance (unit: mm).

Surrounding Rock	The Tunneling	The First Mining	The Second Mining (Distance from Working Face 23205)						
			0 m	10 m	20 m	30 m	40 m	50 m	60 m
Roof	75.29	262.9	462.58	420.07	382.77	353.63	336.93	326.89	312.9
Floor	16.07	64.9	99.91	92.22	86.97	83.55	78.54	75.83	69.62
Pillar sidewall	104.89	563.4	737.07	709.65	671.27	649.67	625.38	614.18	598.86
Mining sidewall	104.89	133.5	216.67	208.09	198.97	186.85	181.65	165.31	159.66

It can be seen from Table 2 that the deformation of the roof, floor, and two sides were 75.29 mm, 11.07 mm, and 104.89 mm, respectively, during double tunneling, and the deformation of the roadway was mainly evident on the two sidewalls.

During the mining of working face 23204, the deformations of the roof, floor, pillar sidewall, and mining sidewall increased by 249.2%, 303.9%, 437.1%, and 27.28%, respectively, compared with the tunneling. The roadway-surrounding rock deformation affected by the first mining was mainly the roof and the pillar sidewall. The deformation of the surrounding rock caused by the first mining was much greater than that of the tunneling.

During the mining of working face 23205, the deformation of the roadway-surrounding rock at the working face changed significantly. The deformation of the roof, floor, pillar sidewall, and mining sidewall increased by 75.9%, 43.2%, 30.8%, and 62.2%, respectively, compared with the first mining. At the same time, the deformation of the roof, floor, pillar sidewall, and mining sidewall gradually increased from 312.9 mm, 69.62 mm, 598.86 mm, and 159.66 mm at 60 m in the front of the working face in 23205 to 462.58 mm, 99.91 mm, 737.07 mm, and 216.67 mm at the head of the working face. The surrounding rock deformation of RAR 23205 affected by the second mining was much greater than that of the tunneling and the first mining; the deformation of the pillar sidewall and roof was especially severe, and the influence of the second mining greatly increased the difficulty of roadway maintenance. Therefore, in order to meet the needs of rapid mining and safe production of the working face, self-moving hydraulic support should be used to support the roof of RAR 23205 in front of the second mining working face.

The deformation and displacement of roadway-surrounding rock at different distances from the front of working face 23205 during the second mining are shown in Figure 14.

According to Figure 14, the displacement of RAR 23205 in the front of the working face decreased gradually with the increase in the distance from the working face. The deformation and failure of the roadway-surrounding rock were mainly caused by horizontal deformation of the pillar sidewall. The displacement of the pillar sidewall reached 737.07 mm, and the roof subsidence was serious. There was no timely support for RAR 23205 in the front of the working face, or the support strength was too low, so the roof was prone to overall subsidence or stepped subsidence at the roadway shoulder corner before the mining of working face 23205.

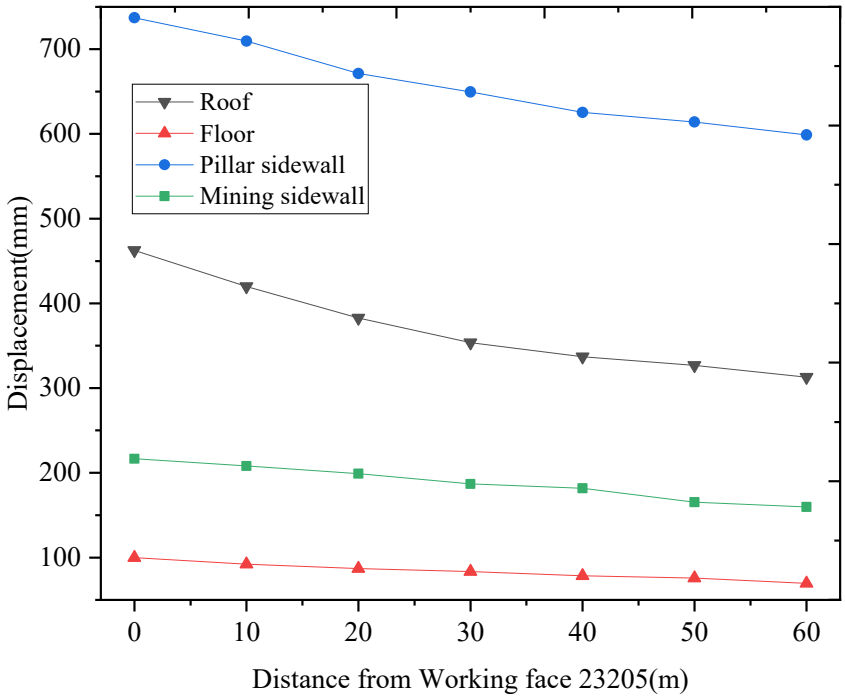

Figure 14. Displacement of the roadway-surrounding rock at different distances from the front of working face 23205 during the second mining.

5. Pressure Relief and Anchorage Control Schemes and Engineering Practice

5.1. Control Technology for Surrounding Rock of Strong Mining Roadways

According to the analysis results on mine pressure behavior, borehole surrounding rock structure detection, mining stress distribution characteristics, and roadway-surrounding rock failure and instability mechanisms of RAR 23204, a pressure relief and anchorage integrated stability control technology is proposed for RAR 23205.

The stress environment of surrounding rock is improved by a pressure relief zone formed by a large-diameter borehole, and the expansion deformation of surrounding rock is absorbed to reduce deformation. At the same time, a short bolt and long cable are used for layered support. The bolts and cables are anchored in different strata. The bolts form a shallow bearing layer in the shallow part of the roadway to prevent the loss and breakage of the shallow coal (rock) body. The cables construct the strengthened bearing layer, which limits the separation of the shallow bearing layer. The shallow and deep bearing layers jointly construct a thick bearing layer of the surrounding rock with high strength and give full play to the bearing efficiency of the surrounding rock of the roadway to limit the deformation of the surrounding rock [28,29].

5.2. Reinforcement Schemes of Strong Mining Roadways

The net width and net height of RAR 23205 are 5.4 m and 3.6 m, respectively. The reinforcement schemes for RAR 23205 are shown in Figure 15.

1. Long anchorage for roof reinforcement

The roof is reinforced by prestressed cable beams consisting of T steel strips of 3200 mm in length and two cables, each Φ17.8 mm in diameter and 6000 mm in length. The spacing of the cables is 3300 mm. The pre-tightening force of the cable is not less than 150 kN.

2. Pillar sidewall reinforcement

The coal pillar is reinforced with one threaded steel bolt, Φ18 mm in diameter and 1800 mm in length. The spacing of the bolts is 1100 mm. The pre-tightening force of the bolt is not less than 60 kN.

3. Mining sidewall reinforcement

The mining sidewall is reinforced by two FRP bolts, each Φ18 mm in diameter and 2000 mm in length. The spacing of the FRP bolts is 1100 mm.

4. Self-moving hydraulic support auxiliary supporting for RAR 23205 in the front of the second mining working face of 23205

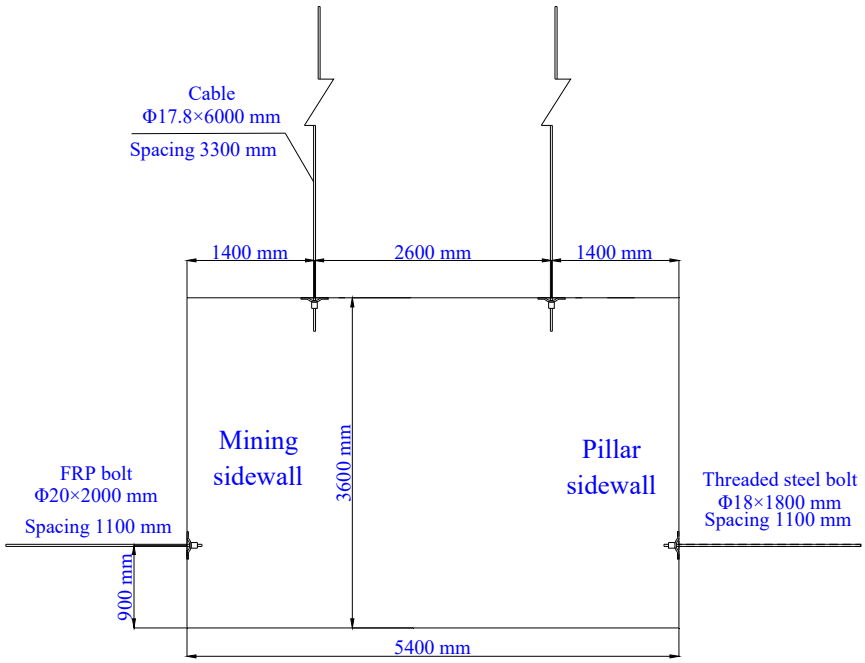

Figure 15. Reinforcement scheme of the strong mining roadway (net section).

RAR 23205 adopts self-moving hydraulic support ZT64000/25/45 for advanced support (Figure 16), and the advanced support distance is not less than 20 m. The jack of the support is in a retractable state under normal conditions. The top beam of the last group of supports is straight with the coal wall, and the support cannot be moved in advance to ensure the support's strength.

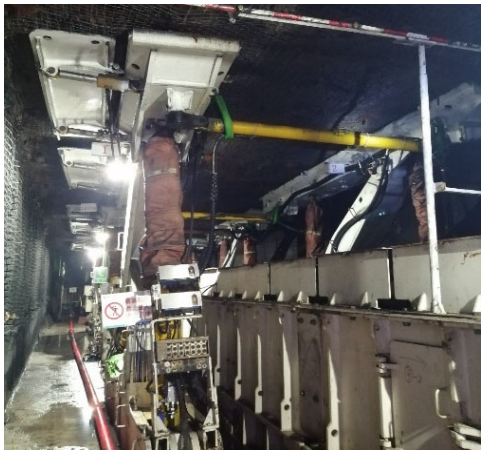

Figure 16. Self-moving hydraulic support.

5.3. Principle and Scheme of Borehole Pressure Relief for Strong Mining Roadways

Due to the stress concentration at the edge of the borehole, the stress in the coal body within a certain range around the borehole is greatly reduced, forming a pressure relief zone. When the pressure relief borehole is reasonably arranged in the coal body, the

pressure relief zones of each borehole are connected and penetrated to form a weakening zone, as shown in Figure 17. The pressure relief borehole destroys the bearing structure of the coal body, and the range of the stress equilibrium zone in the coal body increases significantly. The peak stress shifts to the deep part of the coal body, and the peak stress value of σ_{max} decreases. The coal body, after pressure relief, plays an energy absorption and protection role for the dynamic behavior in the deep coal body and the roof and floor of the roadway. The free space formed by the borehole can absorb the deformation of the roadway-surrounding rock and reduce the influence of dynamic pressure on the roadway.

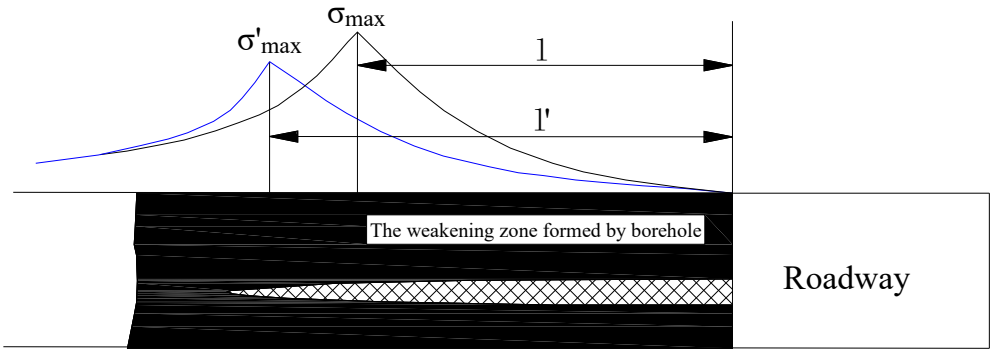

Figure 17. Principle of borehole for pressure relief. The symbols σ_{max} and σ'_{max} are the peak stresses in the roadway sidewalls before and after pressure relief. The symbols l and l′ are the distances from the peak stress to the edge of the roadway sidewall before and after pressure relief.

The pressure relief borehole is arranged in the pillar sidewall (Figure 18), 2000 mm away from the floor; the pillar sidewall arrangement is vertical, and the spacing is 2200 mm. The borehole diameter is 95–125 mm, and the borehole depth is 10 m, as shown in Figure 18. The construction should be completed 20–60 m away from working face 23205 in RAR 23205.

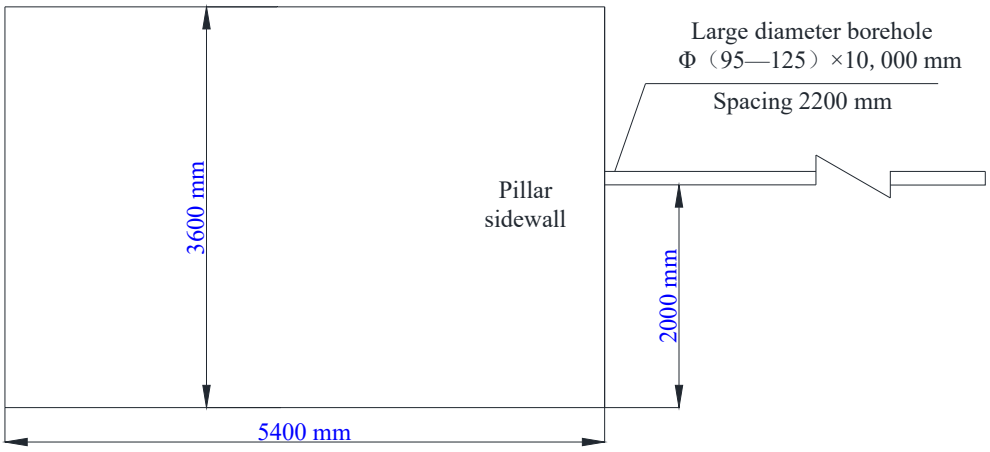

Figure 18. Large-diameter borehole layout (net section).

The drilling rig of ZDY1200L is used for borehole construction (Figure 19). The drilling rig is suitable for roof and roadside boreholes, and the borehole diameter is 95 mm.

In order to explore the development of cracks inside the coal pillar, the integrity of the coal body inside the pressure relief hole is detected and analyzed. Since the diameter of the pressure relief hole is large but the diameter of the imaging instrument probe is only 28 mm, the probe can only capture some of the coal development inside the hole (Figure 20).

Figure 19. Large-diameter borehole drilling rig.

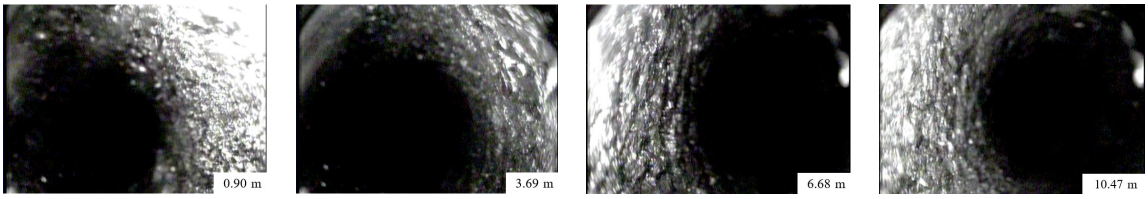

Figure 20. Borehole imaging diagram of the surrounding rock structure of the coal pillar (before the first mining).

According to the surrounding rock detection analysis of a large-diameter borehole in the coal pillar side, there are only a few cracks in some sections, the development crack is small, and the coal structure is relatively complete.

5.4. Evaluation of the Support Effect of a Strong Mining Roadway

5.4.1. Borehole Detection of Surrounding Rock Structure of Strong Mining Roadways

Borehole imager software was used to analyze the borehole detection results of coal–rock fracture separation distribution. The borehole imaging diagram of the roof-surrounding rock structure is shown in Figure 21.

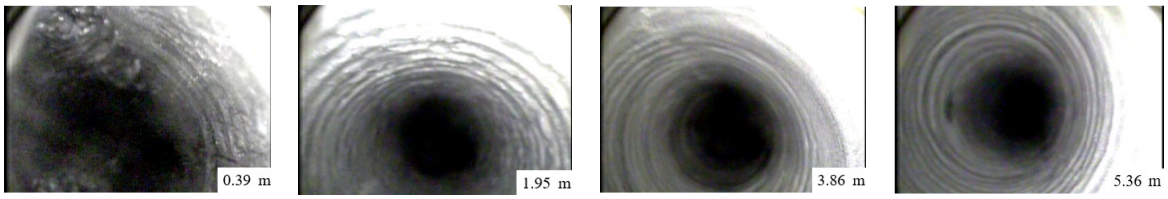

Figure 21. Borehole imaging diagram of the roof-surrounding rock structure.

In Figure 21, we see that there are only a few longitudinal cracks in the shallow roadway roof, and the surrounding rock is complete within 5 m without cracks. Different from the adjacent RAR 23204 affected by mining, the roof crack development is serious, the rock mass is broken, and the roof shows stepped subsidence, so the maintenance of RAR 23205 is better and can meet the requirements of safe and efficient production in coal mines.

5.4.2. Deformation Analysis of Roadway-Surrounding Rock

Through the reinforcement of RAR 23205 before working face 23204 mining, the deformation of the roadway is in a controllable range when the adjacent working face is mined, and the deformation of the surrounding rock is small. Because RAR 23205 lags 100 m behind the working face 23204, the influence of the first mining tends to be stable. At this time, the surrounding rock deformation of RAR 23205 is less than 50 mm and the

roadway is well maintained (Figure 22), which lays the foundation for the second mining and safe production at the working face.

(**a**) (**b**) (**c**) (**d**)

Figure 22. Maintenance effect of RAR 23205: (**a**) pillar sidewall; (**b**) pillar sidewall cracking in some places; (**c**) roof reinforcement with cable beams; (**d**) overall maintenance effect.

6. New Roadways' Layout Optimization and Control Countermeasures

1. The replacement working face adopts the layout of the "H" mining roadway [30], as shown in Figure 23. When working face 1 is being mined, haulage roadway 2 is arranged as a replacement. When haulage roadway 2 is tunneled to the middle of working face 1, it is perpendicular to working face 1 and used to tunnel the central connection roadway. When the central connection roadway is tunneled to the narrow coal pillar of working face 1, working face 1 is completed, and the goaf is stable, the central connection roadway is tunneled along the left and right directions of the narrow coal pillar to form return air roadway 2. This avoids the stress of a second strong mining and can significantly reduce the deformation of the rock surrounding the mining roadway, reduce the size of the protective coal pillar, reduce the waste of coal resources, improve the recovery rate, and ensure the safe, efficient, and sustainable production of the mine;

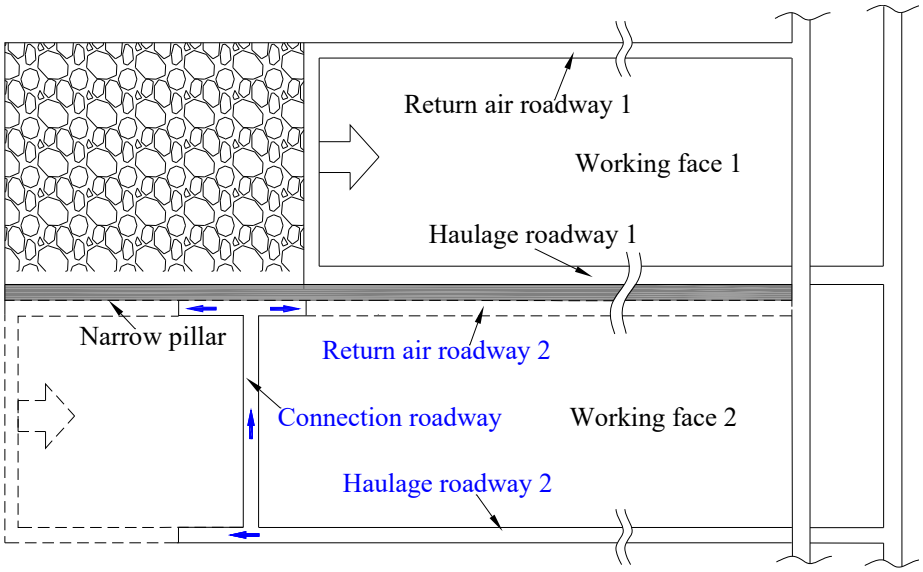

Figure 23. Layout method of the "H" type for mining roadways in longwall coal faces. The blue arrow represents the tunneling direction. The numbers 1 and 2 represent the first and second working faces, respectively.

2. Goaf-side entry driving is adopted, and two or three mining areas are arranged to optimize the mining replacement sequence. The goaf-side entry driving with narrow coal pillars avoids the stress concentration, which is conducive to the stability of roadway-surrounding rock and improves the recovery rate of coal resources [31–33];

3. Increasing the thickness of the anchorage layer in the roof and pre-tightening bolts avoids roof separation in the anchorage zone. A reasonable design of bolt (cable) support parameters and the establishment of double layers of shallow bearing circles and deep strengthening circles can not only control the shallow deformation but also constitute a thick anchoring circle to resist disturbance, and it can give full play to the bearing performance of the roadway-surrounding rock to control the deformation of the surrounding rock [34,35].

7. Conclusions

This paper presents a case study on pressure relief and bolt reinforcement for strong mining roadways in a thick coal seam in Inner Mongolia. It provides a practical reference and guidance for other coal mines with similar geological conditions. Our conclusions are summarized as follows:

1. The factors influencing the large deformation and failure of the rock surrounding a strong mining roadway, i.e., RAR 23204 in Zhuanlongwan Coal Mine, include a large mining height, repeated mining, stress concentration due to a large coal pillar, and a small thickness of the anchorage layer in the roof;
2. The stress evolution of the surrounding rock in RAR 23205 during repeated mining is revealed. The results show that the stress peak in the central coal pillar caused by the first and second mining is 23.19 MPa and 27.49 MPa, respectively, and the stress concentration coefficients are 4.538 and 5.379, respectively. The corresponding distances between the stress peak point and the pillar sidewall are 13 m and 10.5 m, respectively. The deformations of the roadway caused by lateral abutment pressure from the second mining in RAR 23205 are far greater than those of the tunneling and the first mining, and the deformation of the pillar sidewall and roof is especially severe. The influence of the second mining greatly increases the difficulty of roadway maintenance;
3. The countermeasures of pressure relief of large-diameter boreholes in the large coal pillar and long anchorage for roof reinforcement were carried out to control the stability of a strong mining roadway, i.e., RAR 23205. Field measurements indicated that deformations of RAR 23205 in the thick coal seam could be efficiently controlled. The maximum deformation of the surrounding rock of the roadway was 50 mm, which meets the safety and efficiency requirements of the coal mine;
4. Roadways' layout optimization and control countermeasures include adopting the layout mode of the "H" type for new mining roadways and goaf-side entry driving with a narrow coal pillar, increasing the thickness of the anchorage layer in the roof, and pre-tightening the force of bolts. These measures should increase the stability of the rock surrounding strong mining roadways.

Author Contributions: Data curation: D.Q. and J.D.; Formal analysis: J.D.; Funding acquisition: D.Q.; Investigation: D.Q. and J.D.; Project administration: D.Q.; Writing: original draft: D.Q. and J.D.; Writing—editing: D.Q. and J.D.; Writing—review: D.Q., H.J., J.D., J.Y., M.J., G.X., C.Y., Y.Z., J.L., S.H. and B.L. All authors have read and agreed to the published version of the manuscript.

Funding: This work was financially supported by the National Natural Science Foundation of China (grant nos. 51704277, 52074261 and 62204260) and the Fundamental Research Funds for the Central Universities (grant no. 2018QNA27).

Data Availability Statement: Data are contained within the article.

Acknowledgments: The authors would like to express their appreciation to the staff at Zhuanlongwan Coal Mine for their assistance during the field measurements.

Conflicts of Interest: The authors declare no conflict of interest.

Abbreviations

haulage roadway 23204	HR 23204
return air roadway 23205	RAR 23205
return air roadway 23204	RAR 23204
fiberglass-reinforced plastic bolt	FRP bolt

References

1. Huang, B.X.; Zhang, N.; Jing, H.W.; Kang, J.G.; Meng, B.; Li, N.; Xie, W.B.; Jiao, J.B. Large deformation theory of rheology and structural instability of the surrounding rock in deep mining roadway. *J. China Coal Soc.* **2020**, *45*, 911–926.
2. Sun, Y.T.; Li, G.C.; Zhang, J.F.; Xu, J.H. Failure Mechanisms of Rheological Coal Roadway. *Sustainability* **2020**, *12*, 2885. [CrossRef]
3. Yu, H.; Zhang, X.J.; Li, B.Y.; Chu, F.J. Macro-micro mechanical response and energy mechanism of surrounding rock under excavation disturbance. *J. China Coal Soc.* **2020**, *45*, 60–69.
4. Jia, H.S.; Pan, K.; Liu, S.W.; Peng, B.; Fan, K.; Zhuo, J.; Wang, Q. The deformation and failure mechanism and control technology of mining influenced roadway sides. *J. Min. Saf. Eng.* **2020**, *37*, 689–697.
5. Yu, W.J.; Li, K.; Lu, Q.H.; Guo, H.X.; Du, S.H. Engineering characteristics and deformation control of roadways in fractured rock mass. *J. China Coal Soc.* **2021**, *46*, 3408–3418.
6. Zhang, X.D.; Li, Q.W.; Huang, K.Y.; Li, G.X.; Zhang, X. Study of coupling support for large-span coal roadway under mining dynamic load and its application. *Chin. J. Rock Mech. Eng.* **2014**, *33*, 60–68. [CrossRef]
7. Zhao, H.B.; Cheng, H.; Li, J.Y.; Wang, T.; Liu, Y.H.; Qin, F.Y. Study on asymmetric deformation mechanism of surrounding rock of roadway under the effect of isolated coal pillar. *Chin. J. Rock Mech. Eng.* **2020**, *39*, 2771–2784.
8. Jia, H.S.; Pan, K.; Li, D.F.; Liu, S.W.; Fang, Z.Z.; Jin, M. Roof fall mechanism and control method of roof with weak interlayer in mining roadway. *J. China Univ. Min. Technol.* **2022**, *51*, 67–76.
9. Krzysztof, S.; Krzysztof, Z.; Anna, Z.; Derek, B.A.; Wang, J.; Xu, H.; Guo, L. Choice of the arch yielding support for the preparatory roadway located near the fault. *Energies* **2022**, *15*, 3774.
10. Kaiser, P.K.; Yazici, S.; Maloney, S. Mining-induced stress change and consequences of stress path on excavation stability: A case study. *Int. J. Rock Mech. Min. Sci.* **2001**, *38*, 167–180. [CrossRef]
11. Coggan, J.; Gao, F.Q.; Stead, D.; Elmo, D. Numerical modelling of the effects of weak immediate roof lithology on coal mine roadway stability. *Int. J. Coal Geol.* **2012**, *90–91*, 100–109. [CrossRef]
12. Rezaei, M.; Farouq, M.H.; Majdi, A. Determination of longwall mining-induced stress using the strain energy method. *Rock Mech. Rock Eng.* **2015**, *48*, 2421–2433. [CrossRef]
13. Wang, H.W.; Jiang, Y.D.; Xue, S.; Shen, B.T.; Wang, C.; Lv, J.G.; Yang, T. Assessment of excavation damaged zone around roadways under dynamic pressure induced by an active mining process. *Int. J. Rock Mech. Min. Sci.* **2015**, *77*, 265–277. [CrossRef]
14. Osouli, A.; Bajestani, B.M. The interplay between moisture sensitive roof rocks and roof falls in an Illinois underground coal mine. *Comput. Geotech.* **2016**, *80*, 152–166. [CrossRef]
15. Gao, F.Q.; Stead, D.; Kang, H.P. Numerical simulation of squeezing failure in a coal mine roadway due to mining-induced stresses. *Rock Mech. Rock Eng.* **2015**, *48*, 1635–1645. [CrossRef]
16. Luo, Y.; Xu, K.; Huang, J.H.; Li, X.P.; Liu, T.T.; Qu, D.X.; Chen, P.P. Impact analysis of pressure-relief blasting on roadway stability in a deep mining area under high stress. *Tunn. Undergr. Space Technol.* **2021**, *110*, 103781. [CrossRef]
17. Shen, B.; King, A.; Guo, H. Displacement, stress and seismicity in roadway roofs during mining-induced failure. *Int. J. Rock Mech. Min. Sci.* **2008**, *45*, 672–688. [CrossRef]
18. Mo, S.; Tutuk, K.; Saydam, S. Management of floor heave at Bulga Underground Operations. *Int. J. Min. Sci. Technol.* **2019**, *29*, 73–78. [CrossRef]
19. Frith, R.; Reed, G. Coal pillar design when considered a reinforcement problem rather than a suspension problem. *Int. J. Min. Sci. Technol.* **2018**, *28*, 11–19. [CrossRef]
20. Qin, D.D.; Wang, X.F.; Zhang, D.S.; Chen, X.Y. Study on Surrounding Rock-Bearing Structure and Associated Control Mechanism of Deep Soft Rock Roadway Under Dynamic Pressure. *Sustainability* **2019**, *11*, 1892. [CrossRef]
21. Yan, H.; Zhang, J.X.; Feng, R.M.; Wang, W.; Lan, Y.W.; Xu, Z.J. Surrounding rock failure analysis of retreating roadways and the control technique for extra-thick coal seams under fully-mechanized top caving and intensive mining conditions: A case study. *Tunn. Undergr. Space Technol.* **2020**, *97*, 103241. [CrossRef]
22. Xia, Z.; Yao, Q.L.; Meng, G.S.; Xu, Q.; Tang, C.J.; Zhu, L.; Wang, W.N.; Shen, Q. Numerical study of stability of mining roadways with 6.0-m section coal pillars under influence of repeated mining. *Int. J. Rock Mech. Min. Sci.* **2021**, *138*, 104641. [CrossRef]
23. Kajzar, V.; Kukutsch, R.; Waclawik, P.; Nemcikb, J. Innovative approach to monitoring coal pillar deformation and roof movement using 3d laser technology. *Procedia Eng.* **2017**, *191*, 873–879. [CrossRef]
24. Sakhno, I.; Sakhno, S. Numerical studies of floor heave control in deep mining roadways with soft rocks by the rock bolts reinforcement technology. *Adv. Civ. Eng.* **2023**, *2023*, 2756105. [CrossRef]
25. Fang, X.Q.; Guo, M.J.; Lv, Z.Q. Instability mechanism and prevention of roadway under close-distance seam group mining. *Rock Mech. Rock Eng.* **2009**, *28*, 2059–2067.
26. Li, J.Z.; Zhang, J.B.; Hou, J.L.; Wang, L.; Yin, Z.Q.; Li, C.M. Multiple disturbance instability mechanism of dynamic pressure roadway and mining sequence optimization. *J. Min. Saf. Eng.* **2015**, *32*, 439–445.

27. Vardar, O.; Wei, C.C.; Zhang, C.G.; Canbulat, I. Numerical investigation of impacts of geological faults on coal burst proneness during roadway excavation. *Bull. Eng. Geol. Environ.* **2022**, *2*, 101007. [CrossRef]
28. Qian, D.Y.; Deng, J.P.; Wang, S.J.; Yang, X.G.; Cui, Q.; Li, Z.X.; Jin, S.Y.; Liu, W.J. Deformation characteristics and control countermeasures for surrounding rock of deep roadway under mining disturbance: A case study. *Shock. Vib.* **2022**, *2022*, 9878557. [CrossRef]
29. Gao, M.S.; He, Y.L.; Lu, C.P.; Shao, X.; Yang, Z. Coordination mechanism of internal strong active support, soft structure pressure relief and anti-punching of roadway. *J. China Coal Soc.* **2020**, *45*, 2749–2759.
30. Qian, D.Y.; Jiao, H.X.; Cui, Q.; Yang, X.G.; Xian, G.H.; Deng, J.P.; Li, Z.X. A Method of Roadway Layout of H-Type in Coal Mining Face. China Patent No. ZL202111077072.2, 13 September 2021.
31. Kang, H.P.; Zhang, X.; Wang, D.P.; Tian, J.Z.; Yi, Z.Y.; Jiang, W. Strata control technology and applications of non-pillar coal mining. *J. China Coal Soc.* **2022**, *47*, 16–44.
32. Song, Z.Q.; Jiang, J.Q. The current research situation and developing orientation of strata control in coal mine. *Rock Mech. Rock Eng.* **1996**, *15*, 128–134.
33. Zhang, B.S.; Wang, P.F.; Cui, S.Q.; Fan, M.Z.; Qiu, Y.M. Mechanism and surrounding rock control of roadway driving along gob in shallow-buried, large mining height and small coal pillars by roof cutting. *J. China Coal Soc.* **2021**, *46*, 2254–2267.
34. Yao, Q.L.; Li, Y.H.; Xia, Z.; Li, X.H.; Wang, H.H.; Chao, N. Theory and application of roof superimposed beam support of coal roadway based on effective anchorage layer thickness. *J. China Coal Soc.* **2022**, *47*, 672–682.
35. Han, C.L.; Zhang, N.; Kan, J.G.; Ran, Z. Mechanism and application of double active control with pressure-relieving and anchoring for gob-side entry retaining. *J. China Coal Soc.* **2017**, *42*, 323–330.